Cancer Letters 455 (2019) 1–13

Contents lists available at ScienceDirect

Cancer Letters

journal homepage: www.elsevier.com/locate/canlet

Original Articles

CD100-plexin-B1 induces epithelial-mesenchymal transition of head and neck squamous cell carcinoma and promotes metastasis

Chen Zhang[a,2], Hongjiang Qiao[a,2], Weinan Guo[a,2], Yuan Liu[c], Luting Yang[a], Yufeng Liu[a], Boquan Jin[d], Meng Fu[a], Gang Wang[a], Wei Li[a,b,*,1]

[a] Department of Dermatology, Xijing Hospital, Fourth Military Medical University, Xi'an, 710032, China
[b] Department of Dermatology, Huashan Hospital, Fudan University, Shanghai, 200040, China
[c] State Key Laboratory of Military Stomatology & National Clinical Research Center for Oral Diseases & Shaanxi International Joint Research Center for Oral Diseases, Department of Oral Histology and Pathology, Fourth Military Medical University, Xi'an, 710032, China
[d] Department of Immunology, Fourth Military Medical University, Xi'an, 710032, China

ARTICLE INFO

Keywords:
Head and neck squamous cell carcinoma
CD100
Plexin-B1
Snail
Epithelial-mesenchymal transition
Metastasis

ABSTRACT

Head and neck squamous cell carcinoma (HNSCC) is one of the most lethal cancers mainly due to the high rate of metastasis. Here, we find that the expression level of CD100 in HNSCC is positively correlated with the T category, pathological grade and lymph node metastasis of the tumor. The level of soluble CD100 (sCD100) is highly increased in serum of HNSCC patients, and sCD100 markedly induces the epithelial-mesenchymal transition (EMT) of HNSCC through its receptor, Plexin-B1 (PlxnB1), and promotes the metastasis in a xenograft mouse model. Furthermore, sCD100 promotes the stabilization of Snail through the regulation of the Vav1-Rac1/RhoA-p21-activated kinase pathway for the induction of EMT. Anti-CD100 antibody abolishes the CD100-induced EMT and prevents the metastasis of HNSCC, and anti-CD100 antibody also increases the drug sensitivity of HNSCC. Taken together, our study shows for the first time that CD100 induces the EMT of HNSCC and promotes the metastasis, and CD100 would be a candidate as a novel prognostic biomarker and a potential therapeutic target for HNSCC.

1. Introduction

Head and neck squamous cell carcinoma (HNSCC) is the sixth leading cancer worldwide with almost 650,000 new cases diagnosed and 350,000 cancer-related deaths annually [1], which arises from the epithelia of the upper aerodigestive tract, including the oral cavity, oropharynx and hypopharynx [2]. As most HNSCC patients are diagnosed in the late stage with metastasis, the overall survival rate of the tumor is very low [3]. Thus, comprehensive understanding of the precise mechanisms of the metastasis and more efficient targeting therapy are urgently needed.

CD100 (Semaphorin 4D), group IV of the Semaphorins family characterized by steine-rich semaphorin domains, is originally identified based on their ability to provide axon guidance cues during nerve development [4]. CD100 is also expressed in various tumors [4], and is involved in tumor progression, metastasis and suppression [5]. Apart from the membrane form, CD100 can be cleaved by matrix metalloproteinases, resulting in the release of soluble form [6]. PlxnB1 is the high-affinity receptor for CD100 and is highly expressed on epithelial cells. The intracellular structure of PlxnB1 contains Ras GAP and RB domains, which can activate Rho family components [7,8]. Both CD100 and PlxnB1 are expressed in HNSCC tissues and cell lines, and promote the growth and vascularity of tumor xenografts *in vivo* [9]. CD100 also promotes the perineural invasion of HNSCC via the interaction with PlxnB1 expressed on nerves [9]. We find that CD100-PlxnB1 promotes the proliferation and migration of cutaneous SCC cell line A431 and Sa3 [10]. Recruitment of Tiam1 to CD100 activates Rac to enhance the metastasis of oral SCC [11], and CD100-PlxnB1 is also involved in the

Abbreviations: HNSCC, head and neck squamous cell carcinoma; EMT, epithelial-mesenchymal transition; PlxnB1, plexin-B1; sCD100, soluble CD100; GAP, GTPase-activating protein; RBD, Ras-binding domain; DMEM, Dulbecco's modified Eagle medium; H&E, hematoxylin and eosin staining; NAT, normal adjacent tissue; STR, short tandem repeat; Co-IP, co-immunoprecipitation; MMP-2, matrix metalloproteinase-2; PAK1, p21-activated kinase 1

* Corresponding author. Department of Dermatology, Xijing Hospital, 127 Changlexi Road, Xi'an, Shaanxi, 710032, China.
E-mail address: liweiderma@163.com (W. Li).
[1] Present address: Department of Dermatology, Huashan Hospital, Fudan University, Shanghai, 200040, P.R.China.
[2] These authors contributed equally to this work.

https://doi.org/10.1016/j.canlet.2019.04.013
Received 4 November 2018; Received in revised form 8 April 2019; Accepted 8 April 2019

migration of many other tumors [12]. However, the role of CD100 in the metastasis of HNSCC is not clear yet.

Metastasis, the leading cause of death in cancer patients, is closely linked with cell migration, invasion, and epithelial-mesenchymal transition (EMT). EMT is first identified as a developmental process that endows cells that are a part of a rigid architecture to escape and spread [13,14], and later found involved in various biological activities, especially the metastasis of tumors. The gain of mesenchymal markers Vimentin and N-cadherin with a concomitant loss of E-cadherin are hallmarks of EMT. Central to the process of EMT is the increase of the transcription factors of the SNAI family, which leads to the transcriptional repression of E-cadherin and transformation to a mesenchymal phenotype [15–17]. Rho GTPases participate in the regulation of both cadherin-mediated cell-cell adhesion [18,19] and the actin cytoskeleton organization, and is involved in EMT [20]. As CD100 is primarily recognized as a regulator of cell motility, it would be interesting to see whether CD100 is involved in EMT.

In this study, we find that the expression level of CD100 is positively correlated with the metastatic status of HNSCC, and reveal that CD100 is a key inducer of EMT for HNSCC via the regulation of the stability of Snail. We also demonstrate that anti-CD100 antibody abolishes the CD100-induced EMT and inhibits the metastasis of HNSCC. Our results indicate that CD100 might be a novel candidate as a prognostic biomarker and a potential therapeutic target for HNSCC.

2. Materials and methods

2.1. Patients, tumor samples and human HNSCC tissue array and cell lines

The Fourth Military Medical University Ethics Committee approved this study, and informed consent was obtained from the patients before they underwent surgery. Tissue microarray sets including 80 cases of primary HNSCC with follow-up information (Catalog **HN803e**) were purchased from the US Biomax, Inc. The pathological diagnosis and tumor grading of these cases were microscopically reconfirmed by a pathologist. These tissue microarray slides included 61 confirmed cases of HNSCC, 9 normal oral tongues and 2 normal adjacent tissues (NAT), 8 paired lymph node metastases, and their clinical and histological data were provided in Supplementary Tables 1 and 2

For culture of primary human keratinocytes, skin samples were incubated with 2.5 mg/ml Dispase (Gibco, Grand Island, NY, USA) to dissect the epidermis from the dermis, and the separated epidermal tissues were digested with 0.25% trypsin (Hyclone, Little Chalfont, UK) to obtain single cell suspension. The human keratinocyte cell line HaCaT and HNSCC cell line TCA8113 were obtained from the Cell Bank of the Chinese Academic of Sciences (Shanghai, China), and the HNSCC cell line Sa3 and HSQ89 were purchased from the RIKEN Cell Bank (Japan).

2.2. STR analysis

For STR (short tandem repeat) multiplex analysis of the human keratinocyte cell line HaCaT and HNSCC cell lines Sa3, HSQ89, TCA8113, two different multiplex assays were undertaken. The AmpFlSTR IdentifilerH PCR amplification kit that amplifies 15 tetranucleotide repeat loci and the Amelogenin gender-determining marker were obtained from Life Technologies. The PowerPlexH 1.2 System that detects nine loci (eight STR loci and Amelogenin) was obtained from Promega (Mannheim, Germany). STR matching analysis of the obtained STR profile for these cells was done using the online STR analysis provided by the DSMZ (http://www.dsmz.de) and the ATCC STR Profile database for human cell lines (www.atcc.org) that contains 2455 (DSMZ) or 1521 (ATCC) human PowerPlexH 1.2. system-genotyped cell lines. The STR profile of these cells was submitted and deposited in the DSMZ depository. The results were listed in Supplementary Table 3.

2.3. Hematoxylin and eosin staining (H&E)

After fixing tissues in 10% formalin for at least 48 h, the tissues were embedded in paraffin and serial tissue sections (4 μm thick) were cut. The sections were deparaffinized using EZ-DeWaxTM (Bio Genex, San Roman CA, USA) and progressively rehydrated. Afterwards, the sections were stained with hematoxylin and eosin (H&E) staining and examined by a certified pathologist.

2.4. Immunohistochemistry

Immunohistochemical staining was carried out according to the standard protocol (Dakocytomation, USA). The slides were incubated overnight with the following primary antibodies: mouse monoclonal anti-CD100(1:100, **1387543**, BD Transduction Labs), mouse monoclonal anti-PlxnB1(1:200, **A8**, Santa Cruz), rabbit monoclonal anti-RhoA (1:100, **#2117**, Cell Signaling Technology), rabbit polyclonal anti-PAK1 (1:100, **#2602**, Cell Signaling Technology), rabbit monoclonal anti-VAV1 (1:100, **#4657**, Cell Signaling Technology), rabbit monoclonal anti-E-cadherin(1:200, **#3195**, Cell Signaling Technology) and rabbit monoclonal anti-Vimentin(1:200, **#5731**, Cell Signaling Technology). In this study, the number of positively stained cells and the intensity of positive staining were independently scored by two pathologists in a blinded manner. The extended immunoreactivity score standard included (1) the number of cells with positive staining ($\leq$5%: 0; 6–25%: 1; 26–50%: 2; 51–75%: 3; and $>$ 75%: 4) and (2) the staining intensity (colorless: 0; pallide-flavens: 1; yellow: 2; brown: 3). The staining grade was stratified as absent (0 score), weak (1–4 score), moderate (5–8 score) or strong (9–12 score) categories.

2.5. Immunofluorescence analysis

For histo-immunofluorescence analysis, paraffin-embedded tissue sections were deparaffinized and rehydrated with graded ethanol dilutions. After antigen retrieval in Tris-EDTA Buffer (10 mM Tris Base, 1 mM EDTA Solution, 0.05% Tween 20, pH9.0), immunofluorescence staining was performed by incubating the paraffin sections with a primary antibody. For cell-immunofluorescence analysis, the cells were plated on a Glass Bottom Cell Culture Dish (Nest, Wuxi, China) and fixed in 4% paraformaldehyde for 10 min at room temperature. Then the cells were blocked with goat serum and incubated with a primary antibody. The primary antibodies were as the following: rabbit monoclonal anti-E-cadherin (1:200, **#3195**, Cell Signaling Technology), rabbit monoclonal anti-Vimentin(1:200, **#5731**, Cell Signaling Technology), mouse monoclonal anti-CD100(1:100, **1387543**, BD Transduction Labs), rabbit monoclonal anti-Snail (1:100, **#3879**, Cell Signaling Technology) and rhodamine-phalloidin(1:100, CYTOSKELETON). After incubation with the primry antibody overnight at 4 °C, incubation with a secondary antibody (Alexa Fluor 488 Goat anti-rabbit IgG, 1:200, **#4412** Cell Signaling Technology) and (Cy3 Goat anti-mouse IgG, 1:200, **#8890** Cell Signaling Technology) at room temperature was followed for 1 h. DAPI (Dako, Glostrup, Denmark) was used as a counterstain, and analyzed by confocal laser scanning microscopy (FV-1000, Olympus, Tokyo, Japan).

2.6. Small interence RNA preparation, cell transfection and anti-human CD100 antibody

SiRNA oligos against human *PlxnB1*, *CD100, Snail, Vav1, Rac1* and *RhoA* were purchased from GenePharma. PAK1 siRNA was purchased from Santa Cruz Biotechology (**sc-29700**, Santa Cruz, CA). SiRNA transfections were performed using the Invitrogen Lipofectamine siRNAmax Kit according to the manufacturer's instructions. Sequences of the siRNAs were listed in Supplementary Table 4. Prof. Boquan Jin previously established seven hybridoma cell lines secreting monoclonal antibodies against human CD100 [21].

2.7. Quantitative real-time RT-PCR

RNA extraction was performed using the TRIzol Reagent (Invitrogen, Life Technologies, CA, USA) according to the manufacturer's instructions. One microgram of purified RNA fraction was reverse transcribed to cDNA using the PrimeScript™ RT Master Mix kit (Takara, Dalian, China). Quantitative real-time PCR was carried out with a BIO-RAD Multicolor Real-time PCR Detection System (iQTM5) using primers and templates mixed with SYBR Premix Ex Taq II (Takara, Dalian, China). Threshold cycle values were used to calculate the fold change in the transcript levels by using the $2^{-\Delta\Delta CT}$ method. The relative mRNA expression levels were normalized to the *18S* gene. The primer sequences were listed in Supplementary Table 5.

2.8. Western blots analysis

Total protein extracts were obtained using a boiling buffer containing 0.125 M Tris/HCl, pH 6.8, 2.5% SDS and phenylmethanesulfonyl fluoride (protease inhibitor mix; Sigma-Aldrich, St Louis, MO). Nuclear/cytoplasmic fractions were extracted using the CelLytic™ NuCLEAR™ Extraction Kit (*Sigma*) according to the manufacturer's protocol. In all, 30 μg of protein mix was separated by SDS-PAGE and electroblotted onto polyvinylidene fluoride membranes (Millipore, Billerica, MA). The membrane was blocked in 5% non-fat milk TBST for 1 h at 37 °C, followed by incubation with appropriate primary antibodies overnight at 4 °C and then incubated with secondary antibodies for 1 h at room temperature in 5% non-fat milk TBST and visualized by ChemiDOC™ XRS + (Bio-Rad). Primary antibodies were mouse monoclonal anti-CD100 (1:1000, **1387543**, BD Transduction Labs), mouse monoclonal anti-PlxnB1(1:500, **sc-28372**, Santa Cruz, CA), rabbit monoclonal anti-Snail (1:1000, **#3879**, Cell Signaling Technology), rabbit monoclonal anti-RhoA (1:1000, **#2117**, Cell Signaling Technology), rabbit polyclonal anti-RhoB (1:1000, **#2098**, Cell Signaling Technology), rabbit monoclonal anti-RhoC (1:1000, **#3430**, Cell Signaling Technology), rabbit polyclonal anti-Rac1 (1:1000, **#2465**, Cell Signaling Technology), rabbit monoclonal anti-Cdc42 (1:1000, **#2466**, Cell Signaling Technology), rabbit polyclonal anti-Ubiquitin (1:1000, **ab7780,** Abcam), rabbit monoclonal anti-Vimentin (1:1000, **#5741**, Cell Signaling Technology), rabbit monoclonal anti-N-cadherin (1:1000, **#13116**, Cell Signaling Technology), rabbit monoclonal anti-E-cadherin (1:1000, **#3195**, Cell Signaling Technology), rabbit monoclonal anti-ZO-1 (1:1000, **#8193**, Cell Signaling Technology), rabbit monoclonal anti-MMP-2 (1:1000, **#13132**, Cell Signaling Technology), rabbit monoclonal anti-MMP-9 (1:1000, **#13667**, Cell Signaling Technology), rabbit polyclonal anti-PAK1 (1:1000, **#2602**, Cell Signaling Technology), rabbit polyclonal anti-Phospho-PAK1 (Ser204) (1:1000, **#2605**, Cell Signaling Technology), rabbit monoclonal anti-VAV1 (1:1000, **#4657**, Cell Signaling Technology), rabbit monoclonal anti-Phospho-VAV1 (Y174) (1:1000, **ab76225**, abcam), rabbit monoclonal anti-Lamin B2 (1:5000, **#12255**, Cell Signaling Technology), mouse monoclonal anti-Tubulin (1:5000, **CW0098M**, CWBIO, Peking, China) and mouse monoclonal anti-Actin (1:5000, **CW0096M**, CWBIO, Peking, China). Secondary antibodies were goat anti-rabbit IgG (1:5000, **111–035–003**, Jackson ImmunoResearch, West Grove, PA) and goat anti-mouse IgG (1:5000, **115–035–003**, Jackson ImmunoResearch, West Grove, PA). Recombinant human soluble CD100 (*PEPRO TECH* company, Catlog#310–29) was added at the concentration of 300 ng/ml. For signaling pathway inhibition experiments, cells were pretreated with inhibitors targeting RhoA, Rac1 or proteasome (CCG-1423 (300 nM), NSC23766 (50μM), MG132 (10μM), Selleck, Beverly, MA, USA) for 24 h to block these signaling pathways.

2.9. GST-pull down assay

The Sa3 cells were washed with ice-cold PBS rapidly and lysed on ice in 50-mM Tris-HCl (pH 7.4), 1% Triton X-100, 10% glycerol, 2 mM $MgCl_2$, 100 mM NaCl, and protein inhibitor mixture. The lysates were centrifuged at 17,000 × *g* at 4 °C for 5min, and samples were taken from the supernatant to estimate total protein concentration. RhoA activity was determined using Rhotekin RBD beads, and Rac1 activity was determined using PAK-PBD beads. Briefly, 300 μg of clear-cell lysates were incubated with GST-Rho binding domain (RBD) proteins immobilized on glutathione-sepharose beads for 1 h at 4 °C, centrifuged and washed. The active RhoA bound to Rhotekin RBD beads and active Rac1 bound to PAK-PBD beads were eluted in Laemmli sample buffer. GTP-bound Rac1 and RhoA were detected by western blots. The amount of GTP-bound Rac1 and RhoA were normalized to the total amount of the GTP-bound GTPases in cell lysates in each sample separately.

2.10. Wound healing scratch assay

Freshly confluent monolayers of Sa3 cells transfected with the indicated molecules were wounded by manually scraping off cells with a sterile pipette tip. All the wound sizes were verified to ensure that they were all the same width. The cell culture medium was then replaced with serum-free medium containing 4 μg/ml mitomycin C (Sigma, MO, USA), and wound closure was monitored over a 24-h or 48-h period with a phase contrast microscope (Olympus, Tokyo, Japan).

2.11. Cell invasion assay

Cell invasion was assayed using transwell chambers (Costar, Cambridge, MA, USA) with 8-μm pore polycarbonate filters coated with Matrigel™ (BD Biosciences, Franklin Lakes, NJ, USA). And 2.5×10^4 cells (human Sa3 cells and mouse tongue single cell suspensions isolated from WT and CD100 −/− mice) were seeded in the upper well of the transwell chamber, and 10% FBS medium was placed in the lower chamber. Cells on the upper side of the filter were removed after 48 h for the invasion assay. The filter membrane was stained with crystal violet, five fields for each well were counted under the inverted microscope system (Ti-S, Nikon, Tokyo, Japan).

2.12. Apoptosis assay

Cells were scraped from culture dish, and centrifuged at 400 g for 10 min. The cell pellets were then washed by flow buffer (1% fetal bovine serum/PBS) and then stained with PI and Annexin-V for 20 min (BD Biosciences, **559763**, CA). The stained cells were then diluted by binding buffer and analyzed by flow cytometry (FACS Canto II).

2.13. Tumor growth and metastasis assay

In the tumor growth assay, 8×10^6 TCA8113 cells (in PBS) with the indicated transfections were injected subcutaneously into the flank of 5-week-old female nude mice with three mice per group. Tumor size was determined by collecting length and width measurements, and calculating the tumor volume (mm^3) as (tumor length × (tumor width)^2) × 0.52. In the metastatic assay, 8×10^6 cells in a volume of 100 μl were injected into the tail vein of each nude mouse. Mice were killed once they showed signs of sickness and lung and liver were collected and determined by hematoxylin and eosin staining. Slides were analyzed by a pathologist to confirm the presence of metastasis. C57BL6 CD100 KO mice were kindly provided by the RIKEN BRC [6]. All animal study procedures were performed under protocols approved by the Institutional Animal Care and Use Committee of the Fourth Military Medical University.

2.14. Enzyme-linked immunosorbent assays (ELISA)

An in-house optimized sandwich ELISA was established to detect sCD100 in patient serum as reported previously (Liu et al., 2013).

Briefly, ELISA plates (96 wells, Corning Inc, USA) were coated with FMU-CD100–2.4 mAb (10 μg/ml in 0.05 M Na_2CO_3-$NaHCO_3$, pH 9.6) overnight at 4 °C. After washing, the wells were blocked with assay buffer (0.5% BSA in PBS) for 1 h at room temperature. Human CD100-his (Vaccinex Inc, USA) was diluted with assay buffer to set 7 points of diluted standard (25, 12.5, 6.25, 3.125, 1.5625, 0.78125 and 0.390625 ng/ml), and a blank was also included. The standard solution or serum samples were added to the wells (100μl/well) at 37 °C for 1 h. After washing, HRP-conjugated FMU-CD100–2.3 mAb in assay buffer as a detecting antibody was added and incubated at 37 °C for 1 h. TMB (3, 3′, 5, 5′-Tetramethylbenzidine)-substrate (eBioscience Inc, USA) was added to the wells and incubated for 15 min at 37 °C in dark. Absorbance was measured at 450 nm by a plate-reader (BioRad, Hercules, CA, USA).

2.15. In vivo drug sensitivity test

TCA8113 cells (8×10^6) suspended in 200 μl PBS were inoculated subcutaneously in the hind flank of female nude mice (6–8 weeks old). For the anti-cancer drug and antibody treatment experiment, the mice were randomly assigned into experimental or control groups (n = 4 mice/group) once the tumor reached 30 mm^3. Mice in different groups received anti-Ctrl antibody(10 μg/ml), anti-CD100 antibody (10 μg/ml), Celastrol (25 mg/kg body weight) and Celastrol plus anti-CD100 antibody, respectively. Antibodies and Celastrol were given by subcutaneous injection around the tumor region on days 3 and 6 of a 7-day cycle for three cycles. Tumors were measured with calipers every 3 days during the experimental period.

2.16. Co-immunoprecipitation

For the co-immunoprecipitation (CO-IP) assay, all steps were performed at 4 °C. CO-IP was performed with Pierce®Crosslink immunoprecipitation kit. Briefly, AminoLink Plus Coupling Resin was added into the Pierce Spin Columns. 20 μg of mouse monoclonal anti-PlxnB1 antibody (**sc-28372**, Santa Cruz), rabbit monoclonal anti-Snail (**#3879**, Cell Signaling Technology), rabbit monoclonal anti-PAK1 (1:1000, **#2602**, Cell Signaling Technology) or control mouse and rabbit IgG (Beyotime) were added to Protein A/G plus Agarose. Cell lysate was then added into the column and incubated at 4 °C overnight. After centrifugation, elution buffer was added and incubated at room temperature for five minutes. Finally, the flow-through was collected and used for further western blot assay.

2.17. Statistical analysis

Statistical analyses were completed using SPSS 19.0 software (IBM) for Windows. All data shown are mean ± SEM of triplicate values from three separate experiments. $P < 0.05$ was considered to be statistically significant. Independent Student *t*-test or one-way ANOVA were used to compare the continuous variables between the two groups or more than two groups.

3. Results

3.1. Expression level of CD100 in human HNSCC was positively correlated with metastasis grade

Firstly we searched the Oncomine database [22] to see whether the expression level of *CD100* was associated with human HNSCC. Thirty six out of the 112 HNSCC tissues showed increased amplification of *CD100* in the Peng et al. dataset [23] (Fig. 1A), in which the analysis of DNA copy number in HNSCC was independently performed. The TCGA data sheet also showed increased DNA copy number of *CD100* in HNSCC (n = 290) compared with the normal counterpart (blood, n = 338, Fig. 1A). Immunohistochemistry was then performed in the tissue microarray of human HNSCC, and the results showed that the immunoreactivity of CD100 in the metastatic HNSCC (n = 8) was significantly higher than that of the *in situ* HNSCC (n = 61) and normal (n = 9) or NAT (n = 2) ($P < 0.05$, Fig. 1B–C). High-grade (Grades II and III, n = 45) HNSCC had stronger immunoreactivity of CD100 than that of low-grade (Grade I, n = 15) HNSCC ($P < 0.05$, Fig. 1D–E). The expression of CD100 was also higher in T2 (n = 29) and T3 category of HNSCC (n = 16) than that of T1 category (n = 5, $P < 0.05$, Supplementary Fig. 1A and B). A remarkable increase in the CD100 immunoreactivity was noted in the original tumor of the pathological lymph node-positive patient (pN1, n = 20, $P < 0.05$, Supplementary Fig. 1C and D) compared with the pathological lymph node-negative patient (pN0, n = 38). Results of the quantitative realtime PCR (qRT-PCR) and western blots were consistent with the immunohistochemistry data in that the expression of CD100 was higher in the metastatic HNSCC tissues than that of the *in situ* HNSCC (n = 5, $P < 0.05$, Fig. 1F–G). Several cell lines of HNSCC, Sa3, TCA8113 and HSQ-89, also expressed increased level of CD100 compared to HaCaT cells and primary keratinocytes (Fig. 1H–I, Supplementary Fig.1E). The results also showed that the level of sCD100 in the sera of HNSCC patients was about 15-fold higher than in healthy individuals (Fig. 1J).

We also found that the expression level of the receptor for CD100, PlxnB1, was increased in tissues and cell lines of human HNSCC, which was shown in detail in Supplementary Fig.2; however, the expression level of PlxnB1 was not correlated with the metastasis grade (Supplementary Fig.2). Collectively, our data demonstrated that the expression level of CD100 in human HNSCC was positively correlated with the metastasis grade.

3.2. CD100 induced EMT of HNSCC cells

Next we explored the effects of CD100 on the motility of HNSCC cells, and found that sCD100 promoted the migration and invasion of Sa3 and TCA8113 cells in culture, as indicated by cell invasion and wound healing assays (Fig. 2A–B and Supplementary Fig. 3A and B). The effect of sCD100 was greatly reduced when *PlxnB1* was knocked down, indicating that the pro-migratory effect of sCD100 was mediated through PlxnB1 (Fig. 2A–B and Supplementary Fig. 3A and B). Sa3 cells treated with sCD100 exhibited a spindle-like mesenchymal morphology; whereas silencing of *PlxnB1* reversed the cell morphology to an epithelial cobblestone appearance (Fig. 2C). A shrinkable (variable) F-actin fiber length and a cobblestone epithelial shape were also observed in the Sa3 cells treated with PlxnB1-siRNA (Fig. 2D).

Based on the pro-migratory effect and the morphological changes in Sa3 and TCA8113 cells induced by sCD100, we hypothesized that CD100 might trigger EMT, and analyzed the effects of sCD100 on the expression of various EMT-related molecules. The results showed that sCD100 treatment significantly reduced the expression of E-cadherin and ZO-1, and upregulated the expression of N-cadherin, Vimentin, matrix metalloproteinase-2 (MMP-2) and MMP-9. (Fig. 2E–F, Supplementary Fig. 3C and D and Supplementary Fig.4). All the sCD100-induced effects were attenuated when *PlxnB1*was knocked down (Fig. 2E–F, Supplementary Fig. 3C and D and Supplementary Fig.4). Moreover, western blots result showed that the expression of mesenchymal marker was upregulated in tissue of HNSCC (Supplementary Fig.5). These results indicated that CD100-PlxnB1 induced EMT in HNSCC.

To confirm the effects of CD100 on EMT of keratinocytes, we examined the expression of several epithelial and mesenchymal markers in the tongue of CD100 knockout (KO) mice. There was significantly increased expression level of epithelial markers, e. g. E-cadherin, in the tongue of CD100 KO mice compared with that of WT mice (Fig. 2G–H). The expression level of mesenchymal markers, e. g. Vimentin and Snail, was significantly reduced in CD100 KO mice compared with WT mice (Fig. 2G–H). There were less CD100 KO keratinocytes invading through the Matrigel®-coated porous membranes than the WT keratinocytes

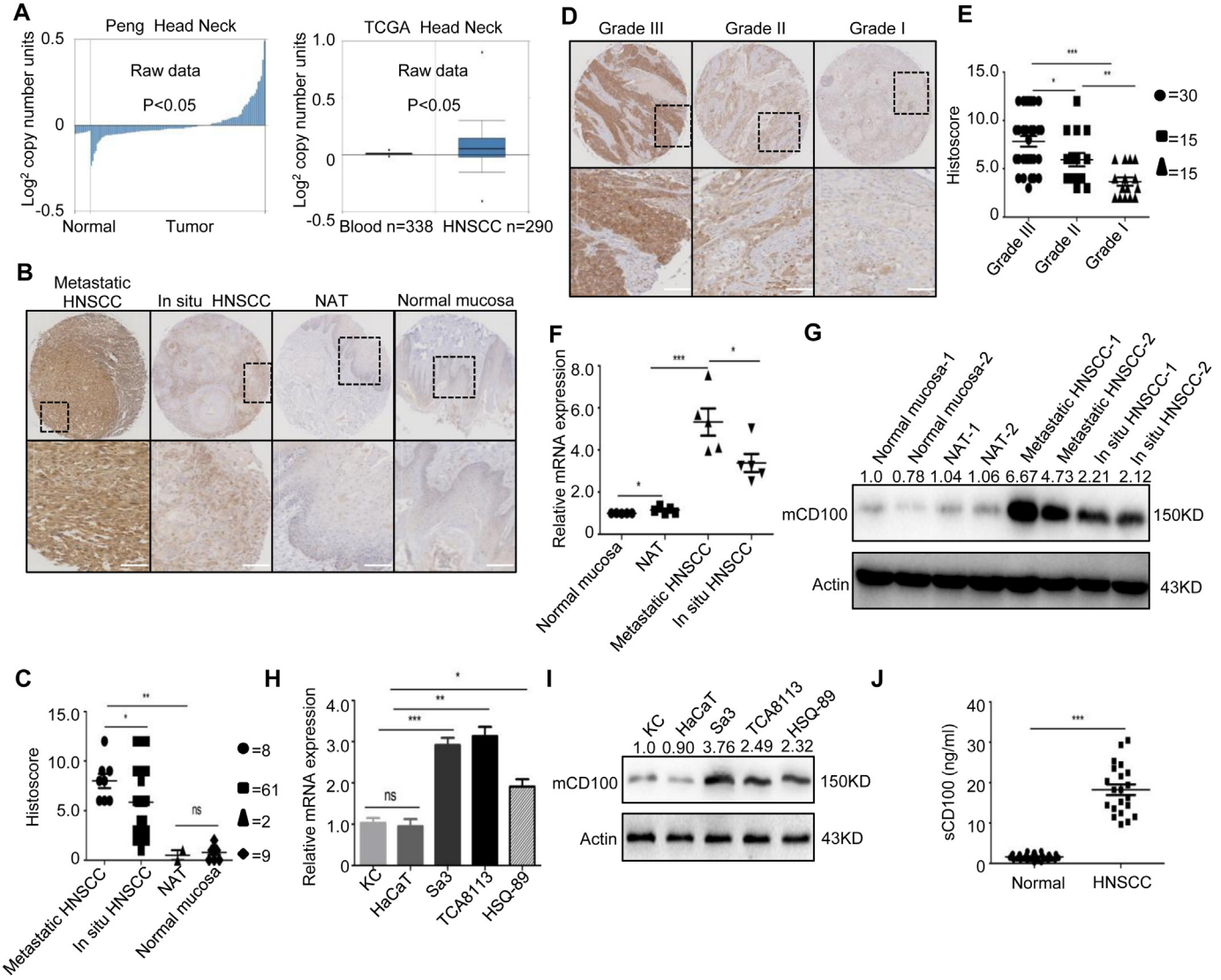

Fig. 1. Expression of CD100 in human HNSCC. (**A**) DNA copy number of *CD100* in HNSCC from Peng's dataset (left) and TCGA head neck cancer dataset (rignt) as shown as raw data. (**B**) Representative immunohistochemistry staining of CD100 in metastatic HNSCC, *in situ* HNSCC, NAT and normal mucosa of oral cavity. (**C**) Quantitative analysis of the immunohistochemistry staining. *ns*, not significant; *, $P < 0.05$; **, $P < 0.01$. Scale bars = 100 μm. (**D-E**) Expression of CD100 in HNSCC with different grades of metastasis (I-III). *, $P < 0.05$; **, $P < 0.01$; ***, $P < 0.001$. Scale bars = 100 μm. (**F-I**) Expression of CD100 in human HNSCC tissues and cell lines was analyzed by qRT-PCR and western blots. *ns*, not significant; *, $P < 0.05$; **, $P < 0.01$. (**J**) ELISA showing the concentrations of sCD100 in sera of HNSCC patients and healthy control subjects. n = 36, ***, $P < 0.001$.

($P < 0.01$, Fig. 2I). Collectively, these data confirmed the effects of CD100 on EMT of keratinocytes in mouse model.

3.3. Stabilization of Snail was required for the CD100-induced EMT

Next, we set out to explore the molecular mechanisms involved in the CD100-induced EMT. Various signaling molecules that had been reported to be related with EMT were screened after sCD100 treatment in Sa3 cells, and it was found that Snail was the most significantly altered molecule compared with Slug, Twist1, Vinculin, Paxillin, Fak, β-catenin, Fbronectin1, Integrin, CD44 and ICAM-1 (Supplementary Fig.6A). The expression level of Snail was correlated with the expression level of CD100 in tissue HNSCC (Supplementary Fig.6B, Supplementary Table 6). Moreover, the level of Snail protein in Sa3 and TCA8113 cells was significantly upregulated after treatment with sCD100, and the expression was downregulated when *CD100* or *PlxnB1*was knocked down (Fig. 3A–B, Supplementary Fig. 6C and D). We examined the level of Snail in cytosolic fraction by western blots using protein extracted from the cytoplasm, and the results showed that Snail protein in Sa3 cell was significantly decreased after treatment with sCD100, and the expression was upregulated when CD100 was knocked down. Meanwhile, the immunofluorescence staining also showed that there were much more staining of Snail in the nucleus in the sCD100-treated cells; however subcellular localization of Snail was out of the nucleus when CD100 was knocked down (Supplementary Fig.7). Furthermore, knockdown of *Snail* abolished the CD100-induced expression of N-cadherin, and increased the expression of E-cadherin and ZO-1, as shown by western blots and immunoflourences staining (Fig. 3C, Supplementary Fig. 8A and B). Knockdown of *Snail* also attenuated the CD100-induced invasion and migration of Sa3 cells (Supplementary Fig. 8C and D). Taken together, these data demonstrated that Snail was the major molecule that mediated the CD100-induced EMT.

In contrast to the significantly changed level of the Snail protein upon treatment with CD100, we detected a mild change in Snail mRNA in Sa3 cells (Fig. 3D), which suggested a post-translational modification of CD100 on Snail. Thus we explored whether CD100 could regulate the degradation of Snail, using cycloheximide (CHX) to block protein

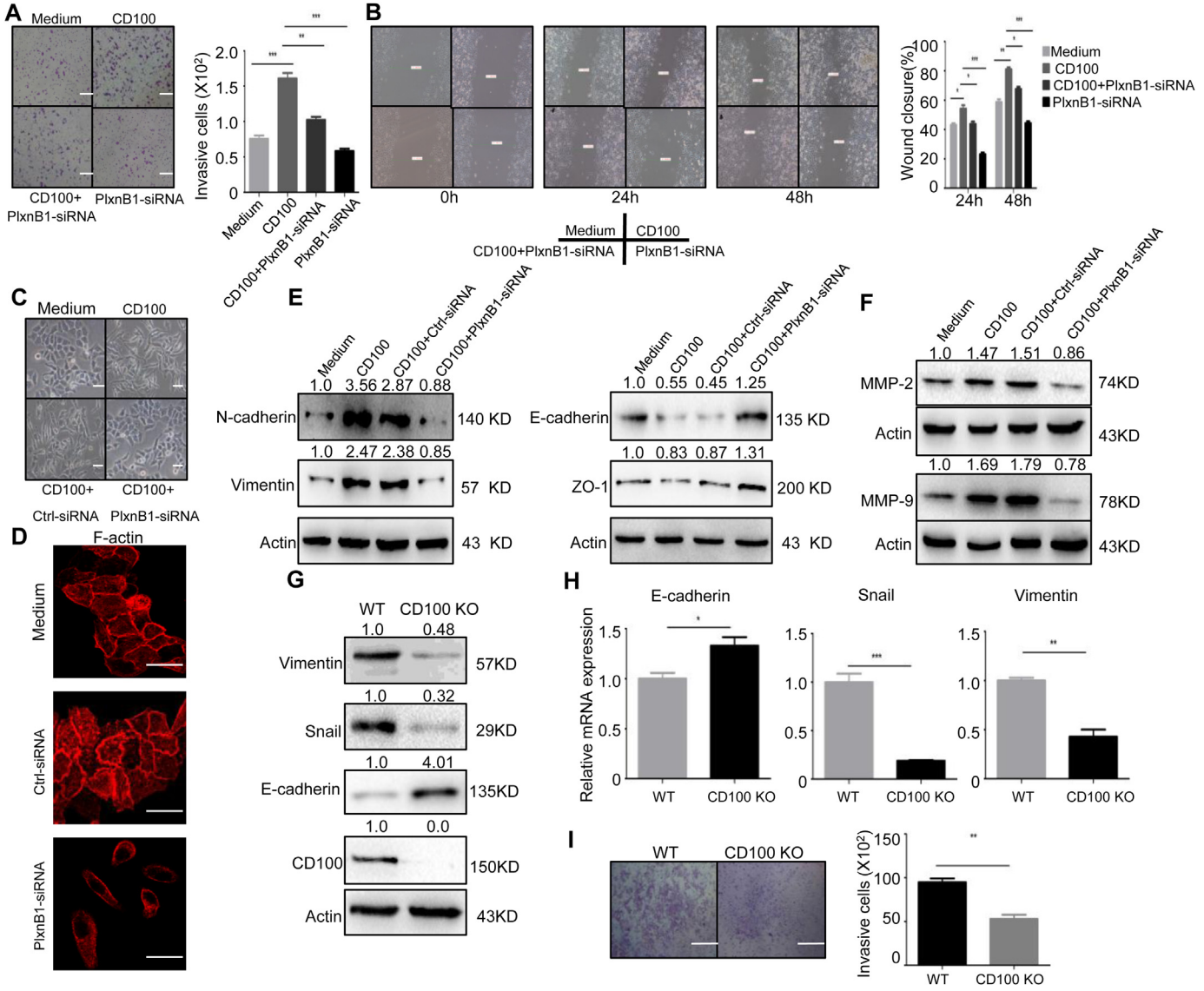

Fig. 2. EMT of HNSCC cells treated with sCD100. (**A-B**) Transwell assay (**A**) and scratch/wound healing assay (**B**) analyzing the effects of sCD100 and (or) PlxnB1-siRNA on invasion/migration of Sa3 cells. (**C**) Phase-contrast microscopy showing the morphological changes of Sa3 cells treated by sCD100. Magnification: 200 ×, scale bar = 100 μm. (**D**) Sa3 cells were treated with PlxnB1-siRNA, and were stained by rhodamine-phalloidin. Magnification: 400 ×, scale bar = 100 μm. (**E**) Western blots showing the expression of EMT markers in Sa3 cells treated with sCD100. (**F**) Western blots showing the expression of MMP-2 and MMP-9 in Sa3 cells treated with sCD100. (**G-H**) Western blots (**G**) and qRT-PCR (**H**) showing the expression of EMT markers in mouse tongue tissues from CD100 KO and WT mice. (**I**) Invasion of single cell suspension from the tongue of CD100 KO and WT mice through the Matrigel®-coated porous membrane. The data are means ± SEM from at least three independent experiments. *, $P < 0.05$; **, $P < 0.01$; ***, $P < 0.001$. All the western blots data shown are representative of at least three independent experiments. Densitometry quantifies the expression levels of EMT markers relative to actin.

synthesis. The results showed that by 4 h, Snail protein was almost completely degraded in control samples (Fig. 3E); however, the degradation of Snail was reduced after treatment with sCD100 (Fig. 3E). Reciprocally, transfection with CD100-siRNA or treatment with anti-CD100 antibody increased the rate of Snail degradation compared with the controls (Fig. 3E). These results indicated that CD100 could regulate the stability of Snail at the protein level. We further demonstrated that treatment with MG132, a proteasome inhibitor, reversed the reduction of Snail in Sa3 cells treated with CD100-siRNA or anti-CD100 antibody (Fig. 3F), indicating that the proteasomal degradation of Snail could be inhibited by CD100. Snail degradation via the proteasome requires ubiquitination, and we found that there was less ubiquitinated Snail in Sa3 cells under the treatment with sCD100; however, treatment with CD100-siRNA induced more ubiquitination of Snail (Fig. 3G). The results of western blots also showed that treatment with MG132 reversed the reduction of Snail treated with CD100-siRNA and increased the induction of Snail in Sa3 cells treated with CD100. The data was shown in Supplementary Fig.9. Collectively, our data showed that CD100 prevented the proteasomal degradation of Snail and increased its stability.

3.4. CD100 activated the Rac1/RhoA pathway for the regulation of EMT

As Rho GTPase pathway functions downstream of PlxnB1, we set out to determine whether the CD100-PlxnB1-medited EMT was through the Rho protein family. The extracts of Sa3 cells were immunoprecipitated with the antibodies against RhoA, RhoB, RhoC, Cdc42 or Rac1, and the results of co-immunoprecipitation showed that PlxnB1 was associated with RhoA and Rac1, but not RhoB, RhoC and Cdc42 (Fig. 4A). Knockdown of RhoA or Rac1 by siRNA increased the expression of E-cadherin and suppressed the expression of Snail and Vimentin in Sa3 cells (Fig. 4B–C and Supplementary Fig.10). And RhoA-

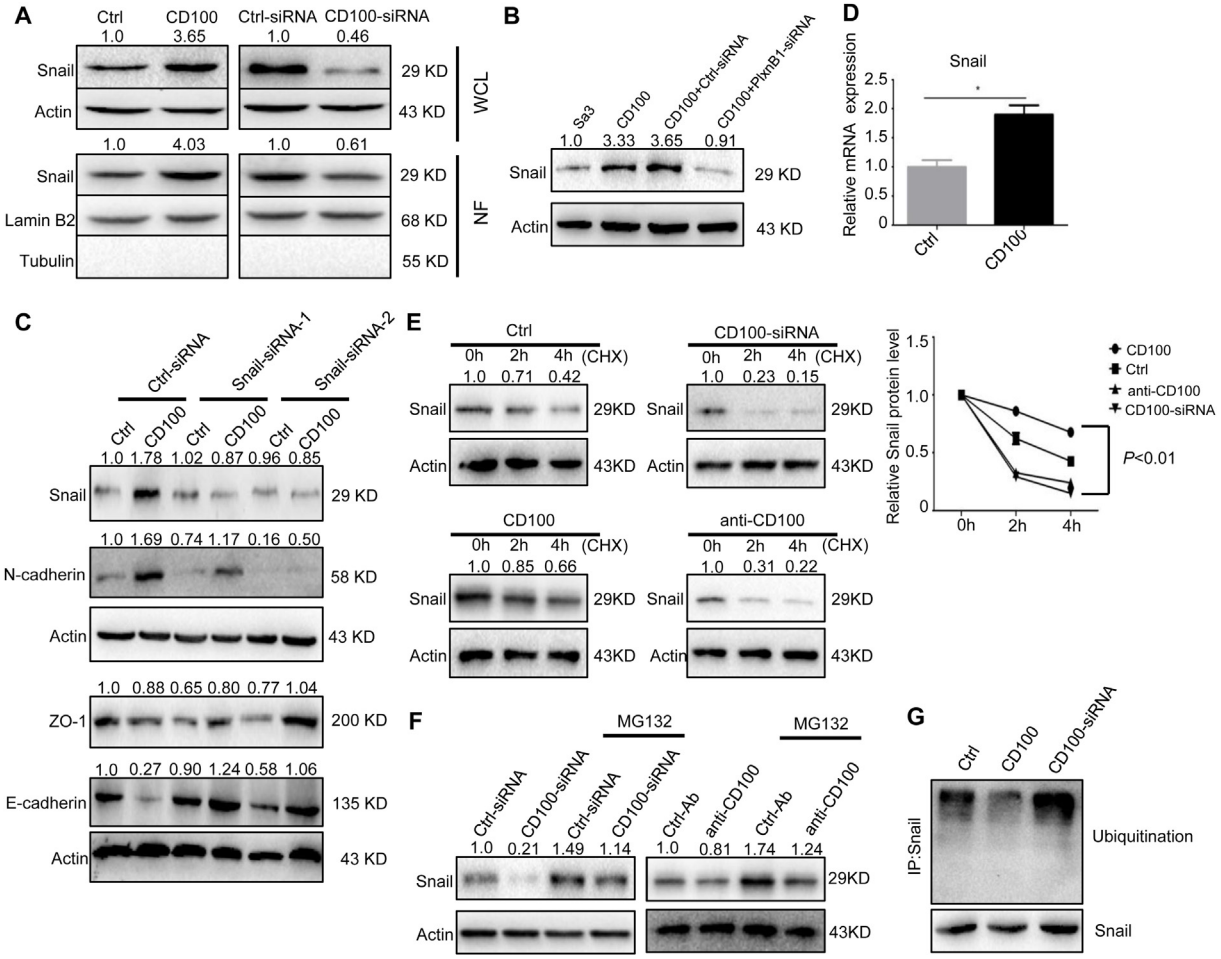

Fig. 3. Expression of Snail in Sa3 cells treated with sCD100. (**A**) Western blots showing the expression of Snail in Sa3 cells treated with either sCD100 (left) or CD100-siRNA (right). Data of the lower panel were obtained from the nuclear fraction of the cells. WCL, wholecell lysate; NF, nuclear fraction. (**B**) Western blots showing the expression of Snail in Sa3 cells treated by sCD100. (**C**) Western blots showing the expression of ZO-1, E-cadherin, Snail and N-cadherin in Sa3 cells treated with sCD100 in the presence of Snail-siRNA or not. (**D**) Results of qRT-PCR showing the expression of Snail mRNA in Sa3 cells treated by sCD100. Data are shown as mean ± SEM from three independent experiments. (**E**) Western blots showing the expression of Snail in Sa3 cells treated with sCD100, CD100-siRNA, or10 μg/ml anti-CD100 antibody. The cells were exposed to 10 μM CHX for 2 h or 4 h before protein extraction. (**F**) Western blots showing the expression of Snail in Sa3 under the treatment of CD100-siRNA or anti-CD100 antibody in the presence of 10 μM MG132 for 24 h. (**G**) Immunoprecipitation of Snail followed by immunoblot for ubiquitination in Sa3 cells treated with sCD100 or CD100-siRNA. *, $P < 0.05$. All the western blots data shown are representative of at least three independent experiments. Densitometry quantifies the expression levels of Snail relative to actin, tubulin or Lamin B2.

or Rac1-silencing abrogated the enhanced invasion and migration of Sa3 cells induced by sCD100 (Fig. 4D, Supplementary Fig.11). These results suggested that Rho GTPase mediated the effect of CD100-PlxnB1 on the EMT of Sa3 cells.

3.5. Activation of the Vav1-Rac1/RhoA-PAK1 pathway by CD100 translocated snail to the nucleus

It's reported that the phosphorylation of Snail by p21-activated kinase 1(PAK1) results in increased nuclear translocation of Snail [24], and PAK1 is regulated by the Rac1-GTPase. Thus we set out to explore whether PAK1 was involved in the CD100-PlxnB1-mediated regulation of Snail. The result showed that the expression level of PAK1 was increased in invasive human HNSCC as indicated by western blots and qRT-PCR (Supplementary Fig.12A), and treatment with PAK1-specific siRNA reduced the protein level of Snail in cultured Sa3 cells (Supplementary Fig. 12B and C). The immunoprecipitation experiment demonstrated that PAK1 and Snail formed a complex in Sa3 cells, which was abrogated by CD100-specific siRNA (Fig. 5A). The Rac1/RhoA-GTP assay further showed the activation of RhoA/Rac1and the phosphorylation of Ser204 in PAK1 and Tyr174 in VAV1, a GTP exchange factor of the Rho GTPase componant [25] (Fig. 5B), which were reduced by the knockdown of CD100 by specific siRNA or inhibition of CD100 activity by anti-CD100 antibody in Sa3 cells (Fig. 5B). We analyzed the activity of RhoA after transfection with Vav1-specific siRNAs by RhoA-GTP assay. We also analyzed the expression of PAK1 by western blots after silencing of RhoA by RhoA-specific siRNAs. The results showed that the activation level of RhoA was significantly reduced in Sa3 cells, and the level of phosphorylation of Ser204 in PAK1 was significantly reduced. Thus our data indicated that Vav1 regulated the activation of RhoA, and RhoA regulated the activation of PAK1. The data were shown in Supplementary Fig.13. Next we found that knockdown of PAK1 by specific siRNA abrogated the sCD100-mediated accumulation of Snail (Fig. 5C). Collectively, our data revealed that CD100 activated the Vav1-Rac1/RhoA-PAK1 pathway in Sa3 cells, which resulted in the nuclear translocation of Snail proteins.

3.6. Silencing of CD100/PlxnB1 suppressed in vivo and in vitro HNSCC metastasis in mouse model and TCA8113 cell line

To verify the effects of CD100 on EMT of *in vivo* HNSCC, we utilized a mouse model of subcutaneous (SC) xenograft tumors of HNSCC.

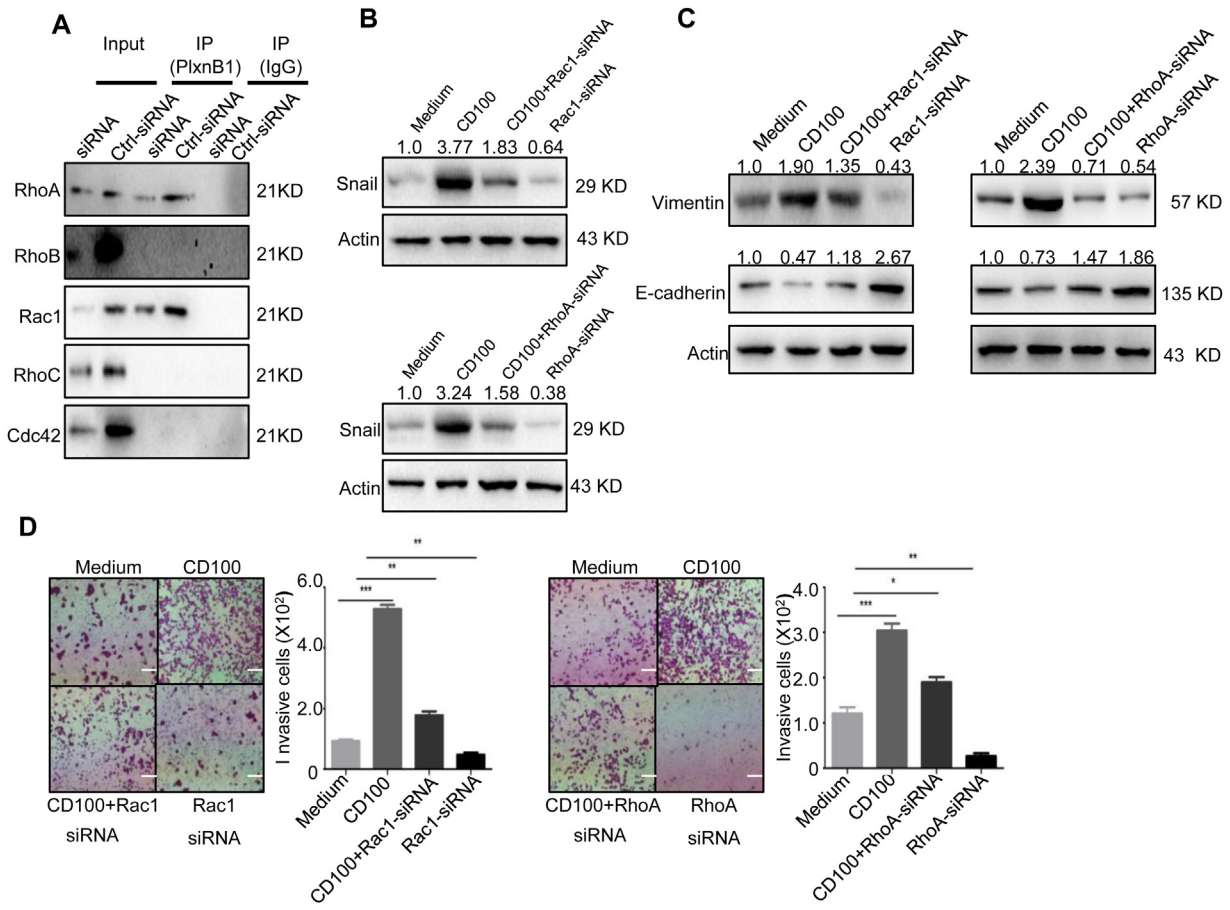

Fig. 4. Activation of Rac1/RhoA pathway in Sa3 cells treated with sCD100. (**A**) Immunoblotting result of Co-Immunoprecipitation assay showing the association of PlxnB1 with RhoA and Rac1, but not RhoB, RhoC and Cdc42 in Sa3 cells. (**B-C**) Western blots showing the expression of Snail, E-cadherin and Vimentin in Sa3 cells under the treatment with sCD100 and (or) RhoA- or Rac1-specific siRNAs. (**D**) Transwell assay analyzing the invasion of Sa3 cells under the treatment with sCD100 and (or) RhoA- or Rac1-specific siRNAs. *, $P < 0.05$; **, $P < 0.01$; ***, $P < 0.001$. All the western blots data shown are representative of at least three independent experiments.

Tumors in mice harboring the TCA8113 cells transfected with PlxnB1-siRNA developed slowlier than that of control (Fig. 6A). At week 6, the average weight and volume of tumors transfected with PlxnB1-siRNA were signifcantly lower than that of control (Fig. 6B–C). The expression levels of PlxnB1 and Ki-67 in tumors transfected with PlxnB1-siRNA were much lower than that of tumors transfected with Ctrl-siRNA (Fig. 6D–E). Moreover, the expression of E-cadherin was higher and expression of Vimentin was lower in tumors transfected with PlxnB1-siRNA than that of Ctrl-siRNA (Fig. 6F–H).

We then assayed whether sCD100 treatment or *CD100*-knockdown could affect the ability of TCA8113 cells to metastasize from the primary tumor site. When injected into the tail vein of mice, the TCA8113 cells transfected with CD100-siRNA developed fewer and smaller tumor nodules in lung compared to the TCA8113 cells treated with Ctrl-siRNA (Fig. 6I, Supplementary Fig.14A). In marked contrast, there were more nodules of tumor cells growing in lung of the mice transferred with the TCA8113 cells treated with sCD100, and the volume of the nodules was bigger (Fig. 6I, Supplementary Fig.14B). Then, the expression of N-cadherin and Vimentin in the lung of the mice transferred with TCA8113 cells treated with sCD100 were analyzed by immunohistochemistry, and the results showed that the expression levels of N-cadherin and Vimentin were significantly increased in the lung of the mice transferred with the TCA8113 cells treated with sCD100 compared with those in the lung of the mice transferred with un-treated TCA8113 cells (Supplementary Fig.15). In clinical samples, we also carried out immunofluorescence analysis on the expression of CD100 and snail in tumor cells surrounding the vessel in HNSCC, and the result showed that the tumor cells highly expressing CD100 also expressed higher level of snail compared with those in healthy controls. The data was shown in Supplementary Fig.16. We also found that sCD100 promoted the stabilization of Snail through regulation of the Vav1-Rac1/RhoA-PAK1 pathway for the induction of EMT in TCA8113 cells by western blots, and the data were shown in Supplementary Fig.17. Then, we analyzed the expression of Vav1, RhoA and PAK1 in metastatic tumors transfected with PlxnB1-siRNA and Ctrl-siRNA by western blots and immunohistochemistry, and the results demonstrated that the expression levels of Vav1, RhoA and PAK1 in tumors transfected with PlxnB1-siRNA were much lower than those of tumors transfected with Ctrl-siRNA, as shown in Supplementary Fig.18. Thus, these data confirmed in *in vivo* and *in vitro* experiments that CD100 promoted the metastasis of HNSCC.

3.7. Anti-CD100 attenuated CD100-induced EMT and increased drug sensitivity

Since sCD100 could induce EMT and promote tumor metastasis, we sought to reverse the EMT process by using anti-CD100 antibody. Our results showed that anti-CD100 antibody inhibited the invasion and migration of Sa3 cells (Fig. 7A–B), and reversed the expression of EMT markers (Fig. 7C–D). When anti-CD100 antibody was applied to the mouse model of xenograft tumors, there was no metastasis in the lung of the mice, and all control antibody-treated mice developed extensive metastases of the tumor (Fig. 7E, Supplementary Fig.19). These data suggested that treatment with anti-CD100 antibody impaired the

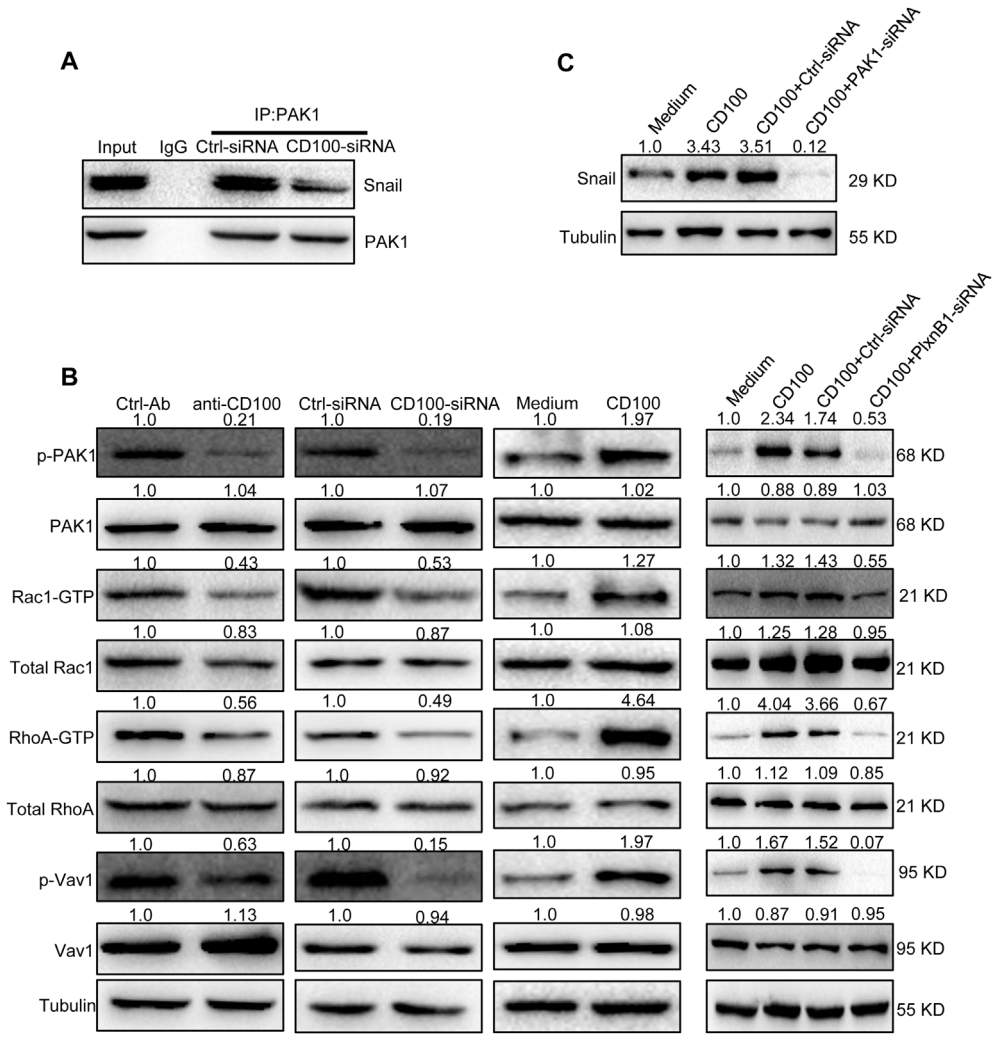

Fig. 5. CD100 activates the Vav1-Rac1/RhoA-PAK1 pathway and translocates Snail to the nucleus. (**A**) Immunoprecipitation of PAK1 followed by immunoblot for Snail in Sa3 cells treated with CD100-siRNA for 24 h. (**B**) Western blots analysis of indicated proteins in Sa3 cells treated with sCD100 or PlxnB1-siRNA and Sa3 cells treated with 10 μg/ml anti-CD100 antibody or transfected with CD100-siRNA. (**C**) Western blots analysis of Snail in Sa3 cells treated with PAK1-siRNA. Data shown are representative of at least three independent experiments. Densitometry quantifies the expression levels of various proteins relative to tubulin.

metastasis of HNSCC.

Then primary HNSCC cells were isolated from three HNSCC patients, for the three clinical tumor cells, the expression level of CD100 were higher than that of Sa3, HSQ-89 and TCA8113, and the result was shown in Supplementary Fig.20. And the tumor cells were incubated with anti-CD100 antibody in the presence or absence of the following anticancer drugs: Triptolide, Celastrol or Triptonide. Anti-CD100 antibody markedly increased the drug sensitivity of HNSCC cells, as demonstrated by the increased rates of apoptosis and decreased level of proliferation in anti-CD100 group (Fig. 8A, Supplementary Fig.21). These *in vitro* results were replicated by *in vivo* xenograft experiment, in which the combination of anti-CD100 antibody with Celastrol significantly inhibited the growth of HNSCC in mice (Fig. 8B–D).

4. Discussion

Metastasis is responsible for the vast majority of deaths of various cancers including HNSCC, and EMT is now considered a hallmark of metastatic cancer and plays a crucial role in metastasis [14,26]. Interaction of CD100 with PlxnB1 regulates the motility of many cell types, and both CD100 and PlxnB1 are highly expressed in HNSCC; thus it's reasonable to speculate that CD100-PlxnB1 might be involved in the EMT of HNSCC. The results of the present study verified our hypothesis and demonstrated that CD100-PlxnB1 induced the EMT of HNSCC, by stablizing the Snail protein via the activation of the Vav1-Rac1/RhoA-PAK1 pathway. Our study also showed that CD100-PlxnB1 promoted the metastasis of HNSCC in the xenograft tumor mouse model, which was consistent with the data from the tumor tissue of HNSCC patients showing that the expression level of CD100 was positively correlated with the metastasis status. Collectively, our study reported for the first time that CD100-PlxnB1 induced the EMT of HNSCC as driving force and promoted the metastasis.

The correlation between CD100 expression and the increased metastasis status of HNSCC is similar to the previous report for other tumors. In colorectal carcinoma tissues, CD100 expression is closely correlated with histological tumor type, tumor-node-metastasis (TNM) stage and lymphatic metastasis [27]. Liu et al. show that CD100 expression is higher in metastatic cervical cancer than that in nonmetastatic cervical cancer [28]. These studies imply that CD100 is involved in metastasis, which heavily relys on cell motility. Actually, CD100 is best known for its role in the development of nervous system [29], by regulating the axon repulsion as a result of the modification of the axonal cytoskeleton at the growing tips or growth cones of axons. The control of axon motility depends critically upon the dynamics of F-actin polymerization and depolymerization, which couples with the regulation of F-actin translocation and microtubule dynamics [30].

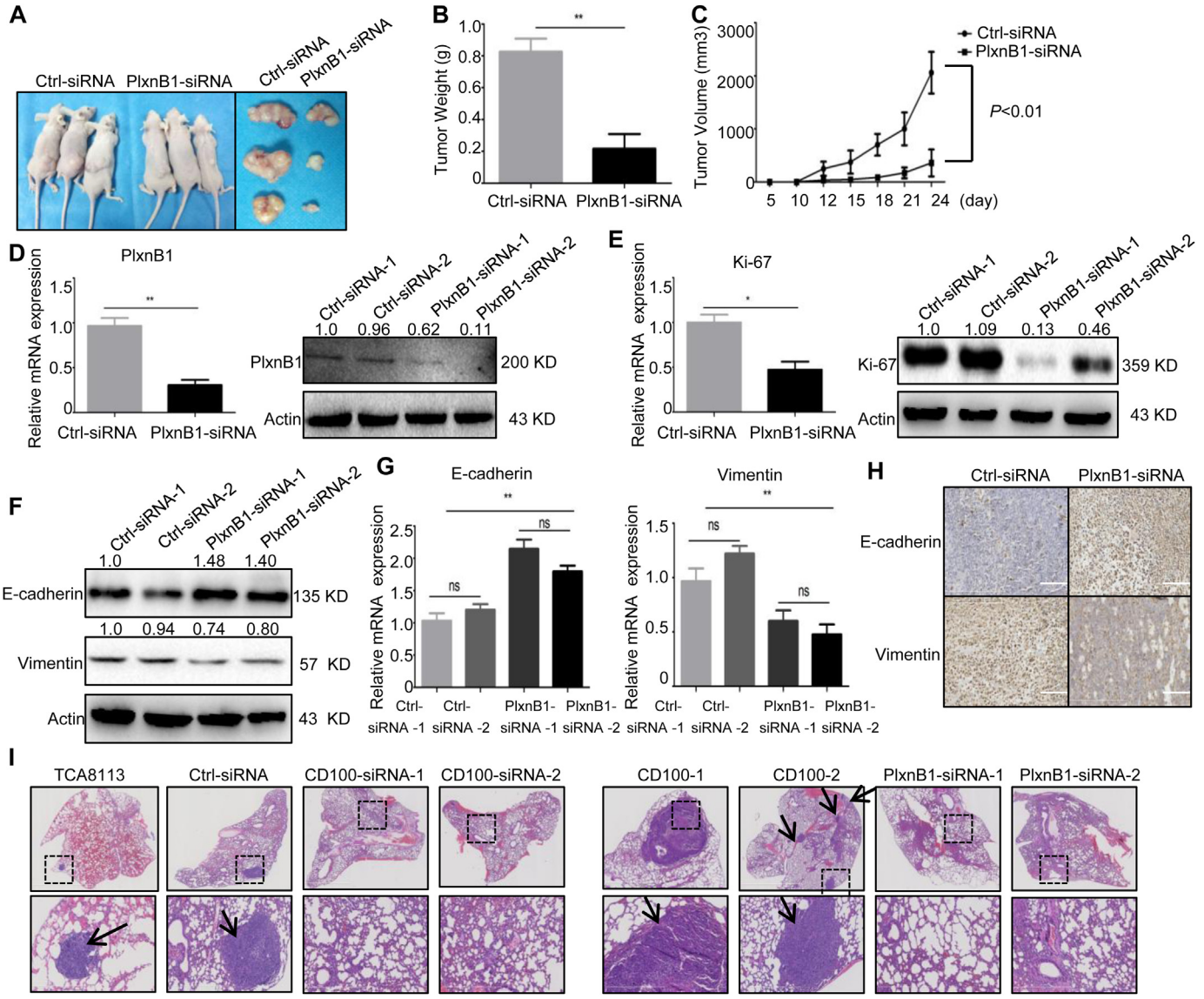

Fig. 6. Silencing of PlxnB1/CD100 suppresseed HNSCC tumor growth and metastasis in a xenograft mouse model. (**A-H**) Nude mice were subcutaneously inoculated with TCA8113 cells transfected with PlxnB1-siRNA, and 42 days later the mice were sacrificed and subjected for analysis on tumor growth and expression of various molecules. Morphologic characteristics, weights and volumes of tumors were shown in (**A-C**). Expression of PlxnB1, Ki-67, E-cadherin and Vimentin at mRNA and protein level were shown by qRT-PCR and western blots respectively (**D-G**). Expression of E-cadherin and Vimentin were shown by immunohistochemistry (**H**). (**I**) Nude mice were injected via the tail vein with the TCA8113 cells transfected with CD100-siRNA or PlxnB1-siRNA, and 42 days later hematoxyin and eosin staining (H&E) of the lung were prepared. Magnification: 200 × ; scale bar = 100 μm *ns*, not significant; *, $P < 0.05$; **, $P < 0.01$. Data shown are representative of at least three independent experiments with at least 3 mice in each group. Densitometry quantifies the expression levels of various proteins relative to actin.

Considering the role of CD100 in the process of cell motility, the close correlation of CD100 with metastasis indicates that CD100 may be involved in EMT. Our data demonstrated that CD100 changed the epithelial cell morphology towards a cancer mesenchymal phenotype, and decreased the expression of epithelial markers and increased the expression of mesenchymal marker. CD100 also influenced the expression of many other molecules involved in the process of EMT. Therefore, we showed for the first time that CD100 induced EMT. The Rho family of small GTPases is centrally involved in the regulation of cytoskeletal dynamics and cell migration and has been extensively studied for its role in invasion and metastasis of cancer cells [31]. The present study showed that the EMT process in HNSCC cancer cells was likely closely related to the activation of Rho GTPase signaling pathway.

The EMT progression is under precise control by various signaling pathways that cooperate to induce full EMT responses. Main intracellular signaling networks such as transforming growth factor (TGF)-β/Smad, integrin/integrin-linked kinase (ILK), and Wnt/β-catenin regulate the EMT by increasing the activity of several transcriptional factors, e. g. Twist, ZEB1, or Snail families, and repressing the expression of E-cadherin and other epithelial cell adhesion proteins [32]. Snail is a zinc finger-type transcriptional repressor, and initiates EMT by repressing epithelial markers and related cell-cell junction proteins while coordinately acting as a major cytoskeletal regulator, and positively correlates with tumor grade, recurrence and nodal metastasis in many types of cancer [33]. Post-translational modifications control the localization, degradation, and thus the activity, of Snail [34]. In our study, we identified that Snail was significantly stabilized by CD100. Indeed, we found that CD100 indirectly triggered a signaling cascade in the phosphorylation and activation of PAK1, which is known to shuttle Snail to the nucleus upon phosphorylation at S246 [24].

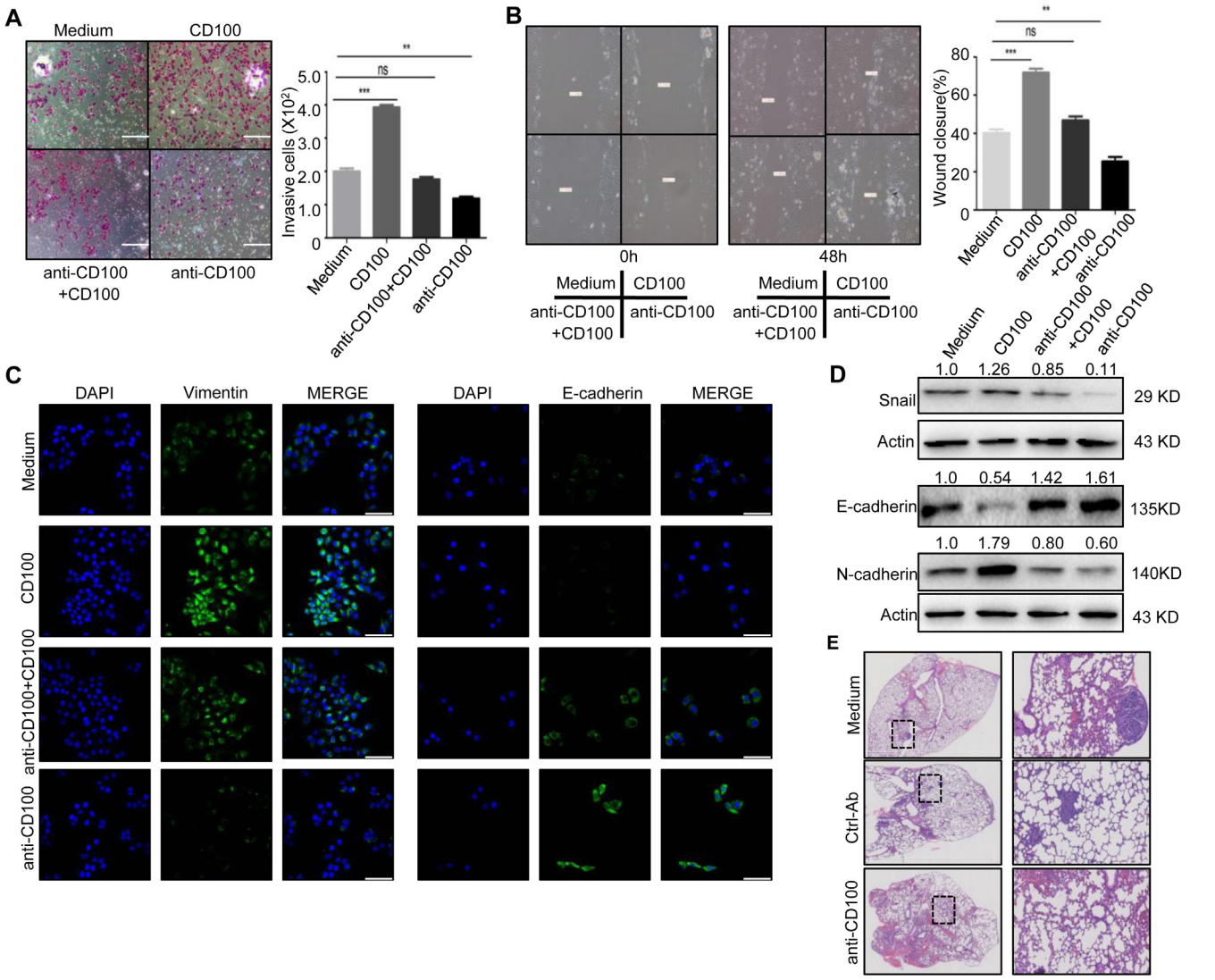

Fig. 7. Migration, EMT and metastasis of HNSCC cells treated with anti-CD100 antibody. (**A-B**) Transwell assay (**A**) and scratch/wound healing assay (**B**) analyzing the invasion/migration of Sa3 cells in the presence of sCD100 and (or) anti-CD100 antibody. Data shown are representative of at least three independent experiments. (**C-D**) Sa3 cells were incubated with sCD100 and (or) anti-CD100 antibody for 48 h. Immunofluorencese staining showed the expression of E-cadherin and Vimentin (green), with the cell nucleus stained with DAPI (blue) (**C**). Magnification: 400 × ; scale bar = 100 μm. Western blots showing the expression of Snail, E-cadherin and N-cadherin (**D**). Data shown are representative of at least three independent experiments. Densitometry quantifies the expression levels of various proteins relative to actin. (**E**) Nude mice were injected via the tail vein with the TCA8113 cells treated with anti-CD100 antibody, and 36 days later H&E staining of the lung were prepared. *ns*, not significant; **, $P < 0.01$; ***, $P < 0.001$. Data shown are representative of at least three independent experiments with at least 3 mice in each group. (For interpretation of the references to color in this figure legend, the reader is referred to the Web version of this article.)

PAK1 and its upstream regulator, the Rac1/RhoA-GTPase, are well-established modulators of cell migration, invasion and metastasis [31]. We found PAK1 was consistently upregulated in the invasive human HNSCC and activated the Rac1-GTPase GTP exchange factor VAV1 by phosphorylation, and we hypothesized that CD100 might be a key upstream regulator of the Vav1-Rac1/RhoA-PAK1 for the Snail cascade. Consistent with this hypothesis, we found that silencing of PAK1 reduced the expression of Snail at the protein level, but not at the mRNA level, and the increase of Snail upon the treatment with CD100 was abrogated when PAK1 was silenced. Importantly, we demonstrated that PAK1 formed a complex with Snail, which was increased under the treatment with sCD100. So we propose that the underlying mechanism by which CD100 regulates EMT is the activation of Vav1-Rac1/RhoA-PAK1-Snail/E-cadherin pathway (Fig. 8E). Data from the present study suggests that CD100 has a positive effect on the stabilization of Snail, and has a negative correlation with the E-cadherin expression. These findings shed light on the understanding of the specific function of CD100 in the regulation of EMT.

CD100 is a multifunctional target involved in a variety of physiological systems, and blocking the activity of this molecule may represent a novel therapeutic strategy. The antitumor drugs may lead to cell damage, which can result in bleb leakage, hypotony, and endophthalmitis [35]. Combination of monoclonal antibody with antitumor drugs not only shows synergistic effect, but also reduces the toxicity of single dose drug. Anti-CD100 antibody binds specifically to CD100 and blocks the binding of CD100 to its receptors, plexinB1, plexinB2, or CD72, and inhibits the downstream physiological effects. The expression of CD100 at the invasive tumor edge creates a barrier for immune infiltration and is inclined to the balance between regulatory and effector immune cells and signals. Actually, antibody-mediated CD100 blockade may open the gate to the tumor and shifts the balance toward anti-tumorigenic immune activity within the tumor [36]. In the present study, our results showed that anti-CD100 antibody enhanced the tumor-killing effect of celastrol. Celastrol is natural

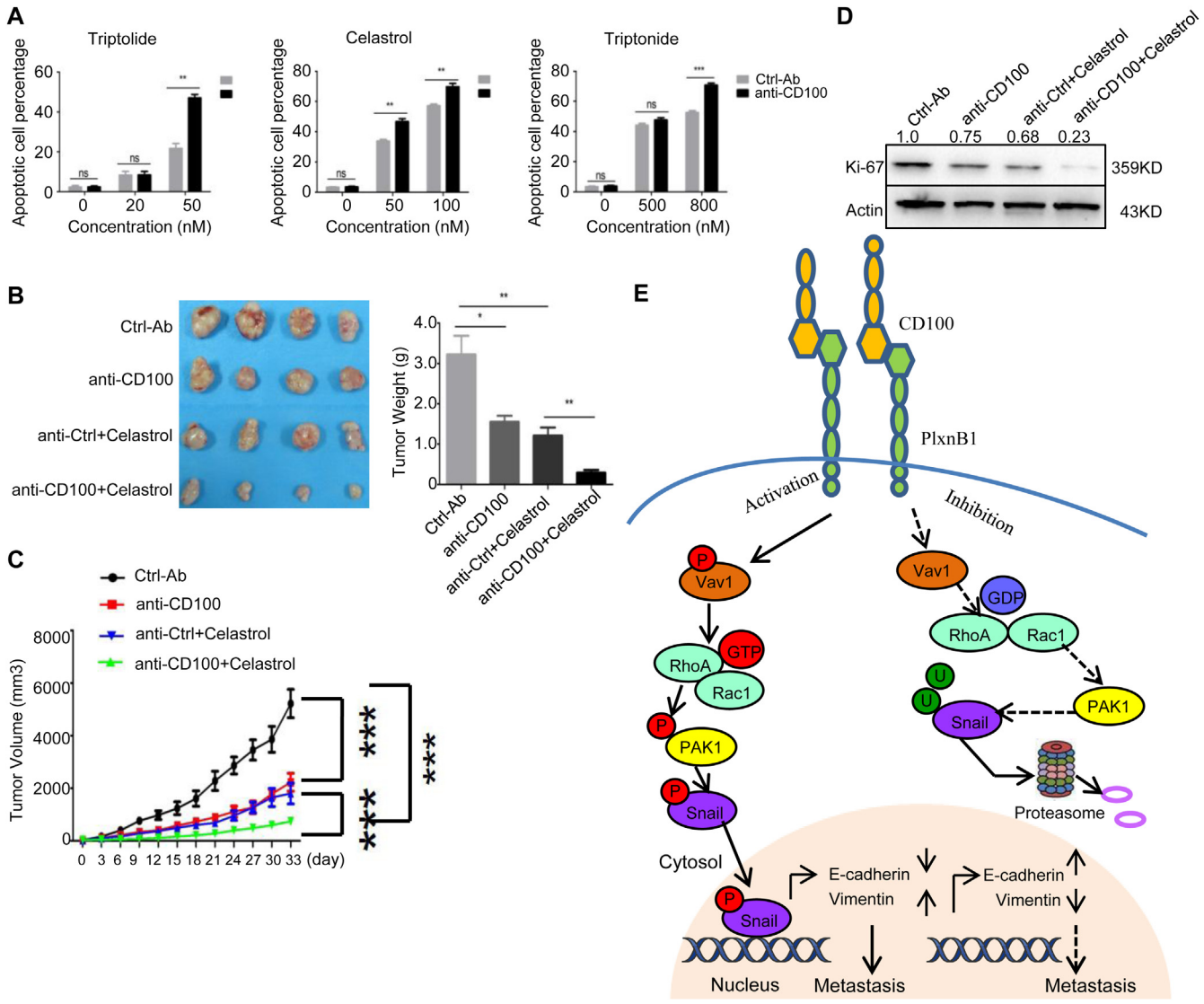

Fig. 8. Drug sensitivity of HNSCC treated with anti-CD100 antibody. (**A**) Primary HNSCC cells were treated with Triptolide, Celastrol or Triptonide in the presence anti-CD100 antibody, and subjected for the analysis of apoptosis. (**B-D**) Nude mice were subcutaneously inoculated with TCA8113 cells, and treated with Celastrol and (or) anti-CD100 antibody for 36 days. Weights and volumes of tumors were shown in (**B-C**). Expression of Ki-67 was shown by western blots (**D**). Data shown are representative of at least three independent experiments with at least 3 mice in each group. Densitometry quantifies the expression levels of various proteins relative to actin. *ns*, not significant; *, $P < 0.05$; **, $P < 0.01$; ***, $P < 0.001$. (**E**) Schematic of proposed pathway for the regulation of Snail by CD100-PlxnB1.

triterpene derived from the Chinese plant Thunder God Vine (*Tripterygium wilfordii*), and exert anti-tumor effects mainly by activating the NF-κB and MMP or PDK1/Akt/mTOR pathway [37,38]. We previously found that sCD100 promoted Akt and Erk phosphorylation in squamous cell carcinoma in a PlxnB1 dependent manner [10], thus anti-CD100 antibody could combine with celastrol to exert synergistic tumor-killing effects.

In conclusion, we demonstrated the clinical significance of CD100 in human HNSCC by showing that CD100 promoted the invasion, metastasis and EMT of HNSCC cells through the recruitment of transcription factor Snail and activation of the Vav1-Rac1/RhoA-PAK1 signaling. CD100 may serve as a therapeutic target in HNSCC therapy.

Conflicts of interest

The authors declare no conflict of interest.

Acknowledgements

We thank Dr James R. McMillan for proofreading of this manuscript. This work was supported by the National Natural Science Foundation of China (81573038, 91642116, 81472885, 81371738); Wei Li was founded by a Municipal Human Resources Development Program for Outstanding Leaders in Medical Disciplines in Shanghai (2017BR039).

Appendix A. Supplementary data

Supplementary data to this article can be found online at https://doi.org/10.1016/j.canlet.2019.04.013.

References

[1] D.A. Gaykalova, J.B. Manola, H. Ozawa, V. Zizkova, K. Morton, J.A. Bishop, et al., NF-kappaB and stat3 transcription factor signatures differentiate HPV-positive and HPV-negative head and neck squamous cell carcinoma, Int. J. Cancer 137 (2015) 1879–1889.

[2] C.R. Leemans, B.J. Braakhuis, R.H. Brakenhoff, The molecular biology of head and neck cancer, Nat. Rev. Canc. 11 (2011) 9–22.
[3] B. Yan, R.V. Broek, A.D. Saleh, A. Mehta, C. Van Waes, Z. Chen, Signaling networks of activated oncogenic and altered tumor suppressor genes in head and neck cancer, J. Carcinog. Mutagen. 7 (2013) 4.
[4] U. Yazdani, J.R. Terman, The semaphorins, Genome Biol. 7 (2006) 211.
[5] A. Kumanogoh, H. Kikutani, Immunological functions of the neuropilins and plexins as receptors for semaphorins, Nat. Rev. Immunol. 13 (2013) 802–824.
[6] W. Shi, A. Kumanogoh, C. Watanabe, J. Uchida, X. Wang, T. Yasui, et al., The class IV semaphorin CD100 plays nonredundant roles in the immune system: defective B and T cell activation in CD100-deficient mice, Immunity 13 (2000) [633]–[642].
[7] L. Tamagnone, S. Artigiani, H. Chen, Z. He, G.I. Ming, H. Song, et al., Plexins are a large family of receptors for transmembrane, secreted, and GPI-anchored semaphorins in vertebrates, Cell 99 (1999) 71–80.
[8] T. Worzfeld, J.M. Swiercz, M. Looso, B.K. Straub, K.K. Sivaraj, S. Offermanns, ErbB-2 signals through Plexin-B1 to promote breast cancer metastasis, J. Clin. Investig. 122 (2012) 1296–1305.
[9] Q. Sun, H. Zhou, N.O. Binmadi, J.R. Basile, Hypoxia-inducible factor-1-mediated regulation of semaphorin 4D affects tumor growth and vascularity, J. Biol. Chem. 284 (2009) 32066–32074.
[10] J. Cao, C. Zhang, T. Chen, R. Tian, S. Sun, X. Yu, et al., Plexin-B1 and semaphorin 4D cooperate to promote cutaneous squamous cell carcinoma cell proliferation, migration and invasion, J. Dermatol. Sci. 79 (2015) [127]–[136].
[11] H. Zhou, M.G. Kann, E.K. Mallory, Y.H. Yang, A. Bugshan, Hua Binmadi NO, et al., Recruitment of Tiam1 to semaphorin 4D activates rac and enhances proliferation, invasion, and metastasis in oral squamous cell carcinoma, Neoplasia 19 (2017) 65–74.
[12] Joanne Soong, Yulin Chen, Elina Shustef, Glynis Scott, Sema4D, the ligand for Plexin B1, suppresses c-Met activation and migration and promotes melanocyte survival and growth, J. Investig. Dermatol. 132 (2012) 1230–1238.
[13] J.P. Thiery, Epithelial-mesenchymal transitions in tumour progression, Nature Reviews 2 (2002) 442–454.
[14] J.P. Thiery, H. Acloque, R.Y. Huang, M.A. Nieto, Epithelial-mesenchymal transitions in development and disease, Cell 139 (2009) 871–890.
[15] W. Huang, X. Cui, J. Chen, Y. Feng, E. Song, J. Li, et al., Long non-coding RNA NKILA inhibits migration and invasion of tongue squamous cell carcinoma cells via suppressing epithelial-mesenchymal transition, Oncotarget 20 (2016) 62520–62532.
[16] A. Hartsock, W.J. Nelson, Adherens and tight junctions: structure, function and connections to the actin cytoskeleton, Biochim. Biophys. Acta 3 (2008) 660–669.
[17] Z.H. Ren, C.Z. Lin, W. Cao, R. Yang, W. Lu, Z.Q. Liu, et al., CD73 is associated with poor prognosis in HNSCC, Oncotarget 20 (2016) 61690–61702.
[18] A. Hall, G.T. Rho, Pases and the actin cytoskeleton, Science 279 (1998) 509–514.
[19] KaibuchiK, S. Kuroda, M. Fukata, M. Nakagawa, Regulation of cadherin-mediated cell-cell adhesion by the Rho family GTPases, Curr. Opin. Cell Biol. 11 (1999) 591–596.
[20] N.A. Bhowmick, M. Ghiassi, A. Bakin, M. Aakre, C.A. Lundquist, M.E. Engel, et al., Transforming growth factor-beta1 mediates epithelial to mesenchymal transdifferentiation through a RhoA-dependent mechanism, Mol. Biol. Cell 12 (2001) [27]–[36].
[21] B. Liu, Y. Ma, J. Yi, Z. Xu, Y.S. Zhang, C. Zhang, et al., Elevated plasma soluble Sema4D/CD100 levels are associated with disease severity in patients of hemorrhagic fever with renal syndrome, PLoS One 8 (2013) e73958.
[22] D.R. Rhodes, S. Kalyana-Sundaram, V. Mahavisno, R. Varambally, J. Yu, B.B. Briggs, et al., Oncomine 3.0: genes, pathways, and networks in a collection of 18,000 cancer gene expression profiles, Neoplasia 9 (2007) 166–180.
[23] C.H. Peng, C.T. Liao, S.C. Peng, Y.J. Chen, A.J. Cheng, J.L. Juang, et al., A novel molecular signature identified by systems genetics approach predicts prognosis in oral squamous cell carcinoma, PLoS One 6 (2011) e23452.
[24] Z. Yang, S. Rayala, D. Nguyen, R.K. Vadlamudi, S. Chen, R. Kumar, PAK1 phosphorylation of snail, a master regulator of epithelial-to-mesenchyme transition, modulates snail's subcellular localization and functions, Cancer Res. 65 (2005) 3179–3184.
[25] J.L. Brown, L. Stowers, M. Baer, J. Trejo, S. Coughlin, J. Chant, Human Ste20 homologue hPAK1 links GTPases to the JNK MAP kinase pathway, Curr. Biol. 6 (1996) 598–605.
[26] M.A. Nieto, The ins and outs of the epithelial to mesenchymal transition in health and disease, Annu. Rev. Cell Dev. Biol. 27 (2011) 347–376.
[27] J.S. Wang, C.Q. Jing, K.S. Shan, Y.Z. Chen, X.B. Guo, Z.X. Cao, et al., Semaphorin 4D and hypoxia-inducible factor-1α overexpression is related to prognosis in colorectal carcinoma, World J. Gastroenterol. 21 (2015) 2191–2198.
[28] H. Liu, Y. Yang, J. Xiao, S. Yang, Y. Liu, W. Kang, et al., Semaphorin 4D expression is associated with a poor clinical outcome in cervical cancer patients, Microvasc. Res. 93 (2014) 1–8.
[29] R.P. Kruger, J. Aurandt, K.L. Guan, Semaphorins command cells to move, Nat. Rev. Mol. Cell Biol. 6 (2005) [789]–[800].
[30] A.B. Huber, A.L. Kolodkin, D.D. Ginty, J.F. Cloutier, Signaling at the growth cone: ligand-receptor complexes and the control of axon growth and guidance, Annu. Rev. Neurosci. 26 (2003) 509–563.
[31] R.J. Pasterkamp, R-Ras fills another GAP in semaphorin signalling, Trends Cell Biol. 15 (2005) 61–64.
[32] Y. Kim, M.C. Kugler, Y. Wei, K.K. Kim, X. Li, A.N. Brumwell, et al., Integrin α3β1-dependent β-catenin phosphorylation links epithelial Smad signaling to cell contacts, J. Cell Biol. 184 (2009) 309–322.
[33] A. Villarejo, Differential role of Snail1 and Snail2 zinc fingers in E-cadherin repression and epithelial to mesenchymal transition, J. Biol. Chem. 289 (2014) 930–941.
[34] H. Peinado, D. Olmeda, A. Cano, Snail, Zeb and bHLH factors in tumour progression: an alliance against the epithelial phenotype? Nat. Rev. Canc. 7 (2007) 415–428.
[35] L.F. Terrence, C.A. Reilly, L.A. Winter, T. Pandina, A. Jonason, M. Scrivens, et al., Generation and preclinical characterization of an antibody specific for SEMA4D, mAbs 8 (2016) [150]–[162].
[36] E.E. Evans, A.S. Jonason Jr., H. Bussler, S. Torno, J. Veeraraghavan, C. Reilly, et al., Antibody blockade of semaphorin 4D promotes immune infiltration into tumor and enhances response to other immunomodulatory therapies, Cancer Immunol Res 6 (2015) 689–701.
[37] X. Sun, X.C. Lin, J.X. Diao, Z.L. Yu, K. Li, Pi (Spleen)-deficiency syndrome in tumor microenvironment is the pivotal pathogenesis of colorectal cancer immune escape, Chin. J. Integr. Med. 22 (2016) 789–794.
[38] Z. Wang, Z. Zhai, X. Du, Celastrol inhibits migration and invasion through blocking the NF-κB pathway in ovarian cancer cells, Exp Ther Med 14 (2017) 819–824.